

Nanofluid flow and heat transfer in boundary layers at small nanoparticle volume fraction: Zero nanoparticle flux at solid wall

J. T. C. LIU*, M. E. FULLER, K. L. WU,
A. CZULAK, A. G. KITHES, C. J. FELTEN

*School of Engineering EN2760
and the Center for Fluid Mechanics
Brown University
Providence, Rhode Island 02912, U.S.A.
e-mail: joseph_liu@brown.edu*

THE CONTINUUM FORMULATION IS APPLIED to the developing boundary layer problem, which approximates the entrance region of nanofluid flow in micro channels or tubes. The thermophysical properties are expressed as “equations of state” as functions of the local nanofluid volume fraction. Based on experimental utilization of nanofluid prevalently at small volume fraction of nanoparticles, a simple perturbation procedure is used to expand dependent variables in ascending powers of the volume fraction. The zeroth order problems are the Blasius velocity boundary layer and the Pohlhausen thermal boundary layer. These are accompanied by the volume fraction diffusion equation. In detailed applications, the boundary condition of zero-volume flux at a solid wall is specified and yields an “insulated wall” solution of constant volume fraction. Two property cases are calculated as comparisons: one is the use of mixture properties for the nanofluid density and heat capacity and the transport properties prevalently used in the literature attributed to Einstein and to Maxwell. Results for alumina are compared to experiments. The theory underestimates the experimental results. This leads to the second comparison, between “conventional” properties and those obtained from molecular dynamics computations available for gold-water nanofluids. The latter properties considerably increased the heat transfer enhancement relative to “conventional” properties and heat transfer enhancement is comparable to the enhanced skin friction rise. To fully appreciate the potential of nanofluids and heat transfer enhancement, further molecular dynamics computations of properties of nanofluids, including transport properties, accompanied by careful laboratory experiments on velocity and temperature profiles are suggested.

Key words: nanofluids, heat transfer enhancement nanoparticles, boundary layers.

Copyright © 2017 by IPPT PAN

*On sabbatical leave, semester I, 2015–16, at the Department of Mechanics and Physics of Fluids, Institute for Fundamental Technological Research, Polish Academy of Sciences, 02-106 Warsaw, Poland. Corresponding author.

1. Introduction

Following an earlier work on the Rayleigh–Stokes solution for nanofluid flow and heat transfer [1], which corresponds to the suddenly accelerated flat plate in its own plane, the present contribution considers the corresponding laminar boundary layer retaining the initial nonlinearity owing to fluid advection. The motivation is for flows with a leading edge where experiments of WEN and DING [2] and JUNG *et al.* [3] show significant heat transfer rate intensification compared to the fully developed regions of nanofluid flow in channels and tubes. The nanofluid is here taken as a base liquid, such as water, seeded with dispersed nano sized particles (of order) 10^{-9} m for purposes of enhancing thermal conductivity and used in micro-sized channels or tubes (of the order 10^{-6} m in width or diameter) for enhancing the surface heat transfer rate in a manner depicted by experiments [2, 3].

The nanofluid is modeled as a liquid containing nanoparticles, small enough so that the nanoparticles are in thermodynamic and momentum equilibrium as if a single fluid. As such, its behavior as a flowing fluid is modeled after a single component “Navier–Stokes fluid”, but that the thermophysical properties are obtained by separate calculations, empirical relations or via measurements pertaining to dilute concentration of nano-sized particles embedded in a base liquid. However, in nanofluids, because of Brownian diffusion due to the bombardment of nanoparticles by the basic liquid molecules, the nanofluid description is supplemented by a diffusion equation for nanoparticle concentration (which is conveniently represented by its volume fraction). This is derivable from the continuity equation for the nanoparticle phase in terms of its mass fraction in the nanofluid. Fick’s Law for the diffusion currents relative to a mass-averaged flow supplements this. The binary diffusion coefficient is then identified with the Brownian diffusion coefficient. Fick’s law is expressed in terms of the nanoparticle mass fraction and is easily converted to that for the volume fraction for small volume fraction. This thought exercise would obtain the diffusion equation presented by BUONGIORNO [4], following the formalism presented by BIRD *et al.* [5] (see also PROBSTEIN [6]). Nanofluid description, however, is inescapable from taking on some aspects of mixture of gases [7].

The general description of nanofluid flow has been applied to boundary layer type flows by PFATSCH [8] who numerically integrated the boundary layer equations. On the basis of prevalent experiments that use small volume concentrations of the nanoparticles, on the order of a few percent or less, a perturbation procedure is devised for the Rayleigh–Stokes problem [1]. While this allows the analytical derivation of perturbation results which aided the interpretation of mechanisms involved in the nanofluid flow and heat transfer, the present work will yield mechanisms of advection versus thermal conduction relevant to the

more involved boundary layer problem. The present contribution considers the laminar boundary layer on a flat plate, which would correspond to the Blasius flow [9] in the absence of nanoparticles, with the perturbation for small volume concentration applied. The accompanying heat transfer problem corresponds to that of POHLHAUSEN [9, 10]. It is not possible to obtain analytical solutions in the manner of the Rayleigh–Stokes problem [1] since the basic Blasius problem requires numerical solution.

2. The general formulation

2.1. The surface heat transfer rate

The surface heat transfer rate, in the boundary layer approximation, is first discussed, as this is the important goal we are after,

$$(2.1) \quad q_0 = -\left(k \frac{\partial T}{\partial y}\right)_0 + (j_p h_p)_0,$$

where q_0 is the surface heat transfer rate, k is the nanofluid thermal conductivity, y is normal to the wall coordinate, j_p is the diffusion current of the nanoparticle phase relative to the mass averaged velocity, h_p is the enthalpy of the nanoparticle phase. Subscript 0 denotes evaluated at the wall surface. Equation (2.1) follows from the more general relation of additional heat transfer mechanism owing to diffusional transport of energy, as is in the case of reacting gases [11].

Fick's Law for the diffusion current with respect to the mass averaged velocity in terms of the nanoparticle phase mass fraction is preferred, as this follows the mass conservation relation of the nanoparticle phase which leads to the diffusion equation. The mass fraction is then related to the volume fraction ϕ and the diffusion current in terms of the volume fraction ϕ becomes

$$(2.2) \quad j_p = -\left(\rho_p D \frac{\partial \phi}{\partial y}\right)_0 + \vartheta(\phi^2),$$

where $\vartheta(\phi^2)$ denotes to the order of ϕ^2 , the binary diffusion coefficient D is identified with that of Brownian diffusion [4], ρ_p is the nanoparticle density. The surface heat transfer rate relation [4] expressed in the present simplified boundary layer form is thus

$$(2.3) \quad q_0 = -\left(k \frac{\partial T}{\partial y}\right)_0 - \left(\rho_p D \frac{\partial \phi}{\partial y} h_p\right)_0.$$

It is observed that while enhanced thermal conductivity directly enhances the surface heat transfer rate, it indirectly stretches out the temperature profile so

that the temperature gradient is lessened. On the other hand, fluid advection of thermal energy helps steepen the temperature gradient. These mechanisms are pointed out even in the much-simplified Rayleigh–Stokes heat transfer problem [1].

2.2. Continuity and momentum equations

The two-dimensional boundary layer equations for steady flow are written in dimensionless form in terms of asterisked quantities. The global continuity equation is

$$(2.4) \quad \frac{\partial \sigma^* u^*}{\partial x^*} + \frac{\partial \rho^* v^*}{\partial y^*} = 0,$$

where the respective dimensionless streamwise and wall-normal coordinates, x^* , y^* are normalized by a streamwise length scale L ; u^* , v^* are the respective dimensionless velocity components normalized by the free stream velocity U . The dimensionless nanofluid density ρ is normalized by the base fluid density with subscript f , $\rho^* = \rho/\rho_f$. The zero-pressure gradient streamwise momentum equation is

$$(2.5) \quad \rho^* \left(u^* \frac{\partial u^*}{\partial x^*} + v^* \frac{\partial u^*}{\partial y^*} \right) = \frac{1}{\text{Re}} \frac{\partial}{\partial y^*} \left(\mu^* \frac{\partial u^*}{\partial y^*} \right).$$

$\text{Re} = UL/\nu_f$ is the Reynolds number based on fluid kinematic viscosity, $\nu_f = \mu_f/\rho_f$, μ_f is the fluid viscosity coefficient. The nanofluid viscosity coefficient μ is made dimensionless as $\mu^* = \mu/\mu_f$. The wall-normal momentum equation reduces to zero-pressure gradient across the boundary layer.

2.3. Thermal energy equation

The energy equation is similar to that for a reacting gas in that the heat flux vector would include heat transport of thermal energy by diffusion currents. The generic convective heat transfer equation follows from the first law of thermodynamics in differential form. For the steady two-dimensional boundary layer, written first in dimensional form

$$(2.6) \quad \rho u \frac{\partial h}{\partial x} + \rho v \frac{\partial h}{\partial y} = - \frac{\partial q}{\partial y},$$

where $h = \int c dT$ is the static enthalpy of the nanofluid, T is the temperature, c is the nanofluid heat capacity $c = dh/dT$. The energy equation is in the incompressible form for low Mach numbers (i.e., where the Mach number $M \rightarrow 0$) and small temperature loading. For low Mach numbers, the work owing to pressure

gradients and the rate of viscous dissipation are negligible as these effects are proportional the square of the Mach number (see LAGERSTROM [12]). The small temperature loading allows taking the thermophysical properties to be temperature independent. However, properties such as ρ , c , and transport coefficients are nanofluid volume concentration dependent.

The boundary layer form of q in the interior of the nanofluid is

$$(2.7) \quad q = -\left(k \frac{\partial T}{\partial y}\right) - \left(\rho_p D \frac{\partial \phi}{\partial y} h_p\right).$$

Inserting (2.6) into (2.5), the dimensionless energy equation then takes the form

$$(2.8) \quad \rho^* c^* u^* \frac{\partial \theta}{\partial x^*} + \rho^* c^* v^* \frac{\partial \theta}{\partial y^*} \\ = \frac{1}{\text{Re Pr}_f} \frac{\partial}{\partial y^*} \left(k^* \frac{\partial \theta}{\partial y^*} \right) + \frac{\phi_\infty}{\text{Re Sc}_f} \frac{\partial}{\partial y^*} \left(\rho_p^* D^* \frac{\partial \Phi}{\partial y^*} c_p^* \theta \right),$$

where the dimensionless volume fraction is defined as $\Phi = \phi/\phi_\infty$, ϕ_∞ is the volume fraction in the free stream, $D^* = D/D_{ref}$, where for Brownian diffusion [4] $D = k_B T / 6\pi\mu_f r_d$, k_B is the Boltzmann constant, r_d is the nanoparticle radius (or averaged radius), $D_{ref} = k_B T_{ave} / 6\pi\mu_f r_d$, T_{ave} is an averaged temperature. The dimensionless temperature is $\theta = (T - T_\infty) / (T_0 - T_\infty)$. The base fluid Prandtl and Schmidt numbers are, respectively, $\text{Pr}_f = \nu_f / \alpha_f$ and $\text{Sc}_f = \nu_f / D_{ref}$, the base fluid thermal diffusivity is $\alpha_f = k_f / \rho_f c_f$, c_f is the base fluid heat capacity, k_f is the base fluid thermal conductivity. Other dimensionless quantities are defined $\rho^* = \rho_p / \rho_f$, $c_p^* = c_p / c_f$, and $c^* = c / c_f$. The subscript p denotes that of the nanoparticle material.

The ‘‘incompressible’’ approximation of low Mach numbers and small relative temperature differences rendered the transport coefficients to become temperature independent if the double expansion procedure suggested in LAGERSTROM [12] is carried out. Similar to the viscosity coefficient and thermal conductivity in this case, the Brownian diffusion coefficient, though it is explicitly expressed as a linear function of the temperature, is taken as constant so that as long as the nanoparticles are indeed dilute, the dimensionless Brownian diffusion coefficient D^* is unity.

2.4. Mass diffusion equation

The volume fraction diffusion equation, which follows from the nanofluid mass conservation equation, supplemented by Fick’s Law already discussed, is

$$(2.9) \quad u^* \frac{\partial \Phi}{\partial x^*} + v^* \frac{\partial \Phi}{\partial y^*} = \frac{1}{\text{Re Sc}_f} \frac{\partial}{\partial y^*} \left(D^* \frac{\partial \Phi}{\partial y^*} \right).$$

The effects of thermal diffusion, which has been estimated to be small relative to mass (volume fraction) diffusion [4], is neglected at the outset, as well as its effect on energy transport in the energy equation.

2.5. The boundary conditions

The physical boundary conditions, in terms of the dimensionless variables, are

$$(2.10) \quad \begin{aligned} y^* = 0 : u^* = 0, \theta = (T - T_\infty)/(T_0 - T_\infty) = 1, (\partial\Phi/\partial y^*) = 0 \text{ or } \Phi = \Phi_0, \\ y^* = \infty : u^* = 0, \theta = 0, \Phi = 1. \end{aligned}$$

There are two general boundary conditions in (2.10) for the volume fraction (Buongiorno, private communication 2010): In the present work the solid wall is assumed impermeable to nanoparticles. The zero-flux boundary condition would yield, from the diffusion equation, a constant volume fraction throughout the boundary, $\Phi(x^*, y^*) = 1$, as solution in absence of thermal diffusion and nanoparticle sources (or sinks). In this case, the surface heat transfer rate (2.3) is accomplished by thermal conduction alone. The wall boundary condition for the temperature is the familiar one for the heat transfer problem by imposing a constant temperature for which the surface heat transfer rate is sought.

3. Thermophysical properties

Thermal conductivity and viscosity of nanofluids has been the subject of discussion and measurements by large groups of authors and laboratories (BUONGIORNO *et al.* [13], VENERUS *et al.* [14]). The density and heat capacity of nanofluids, of essential interest in continuum description of nanofluid flows, on the other hand, are prevalently obtained as if the nanoparticles and base fluid were a mixture of gases. Only gold nanofluid density and heat capacity are obtained systematically from molecular dynamics computations (PULITI [15], PULITI *et al.* [16]). For recent review of nanofluid properties, one is referred to PAOLUCCI and PULITI [17].

The intention here is to obtain specific forms of the properties for the two situations in which the present theory will be applied:

- (1) water-based alumina nanofluid for which there are entrance region experiments [2, 3] to compare with the present boundary layer theory and,
- (2) water-based gold nanofluid for which thermophysical property results are available from molecular dynamics [15–17] and this can be compared to boundary layer results using mixture theory for the nanofluid density and heat capacity and classical theory for the nanofluid intrinsic viscosity (Einstein) and thermal conductivity (Maxwell).

3.1. Density and heat capacity

In general, nanofluid properties are expressed as a function of the volume fraction ϕ . Most, if not all, relevant heat transfer enhancement experiments using nanofluids are performed for $\phi \ll 1$. In this case, we are interested in expressing nanofluid properties in the form

$$(3.1) \quad \begin{aligned} \rho^* &= \rho/\rho_f = 1 + \phi_\infty (\rho^*)'_{\phi=0} \Phi_1 + \vartheta(\phi_\infty^2), \\ \rho^* c^* &= \rho c/\rho_f c_f = 1 + \phi_\infty (\rho^* c^*)'_{\phi=0} \Phi_1 + \vartheta(\phi_\infty^2), \end{aligned}$$

where $\Phi_1 = \phi_1/\phi_\infty$ is the first order dimensionless volume fraction, the slope of the respective properties $(\rho^*)'_{\phi=0}$, $(\rho^* c^*)'_{\phi=0}$ are obtained from mixture expressions but preferably from rarely available molecular dynamics computations or measurements. In the case of mixture mimicking,

$$(3.2) \quad \begin{aligned} (\rho^*)'_{\phi=0, mix} &= \rho_p^* - 1, \\ (\rho^* c^*)'_{\phi=0, mix} &= \rho_p^* c_p^* - 1, \end{aligned}$$

where $\rho_p^* = \rho_p/\rho_f$, $\rho_p^* c_p^* = \rho_p c_p/\rho_f c_f$, are the nanoparticle material density and density-heat capacity product made dimensionless by that of the base fluid. In the mixture calculation, ρ^* and $\rho^* c^*$ are identical linear functions of the volume fraction.

3.2. Transport properties

The dimensionless nanofluid viscosity coefficient and heat conductivity are also written as ascending powers of the volume fraction,

$$(3.3) \quad \begin{aligned} \mu^* &= \mu/\mu_f = 1 + \phi_\infty (\mu^*)'_{\phi=0} \Phi_1 + \vartheta(\phi_\infty^2), \\ k^* &= k/k_f = 1 + \phi_\infty (k^*)'_{\phi=0} \Phi_1 + \vartheta(\phi_\infty^2). \end{aligned}$$

One is referred to recent reviews of transport properties of nanofluids [13, 14, 17, 18]. The diffusion of nanoparticle concentration is here taken to be from Brownian motion [4].

4. Perturbation analysis for small nanofluid volume concentration,

$$\phi_\infty \ll 1$$

The thermophysical properties, expressed as function to first order in ϕ are already in a form suitable for perturbation expansion: The zeroth order is the base fluid devoid of nanoparticles. The nanofluid flow quantities are expanded

ascending powers of $\phi_\infty \ll 1$, with asterisks omitted for simplicity,

$$(4.1) \quad \begin{aligned} u &= u_0 + \phi_\infty u_1 + \vartheta(\phi_\infty^2), \\ \theta &= \theta_0 + \phi_\infty \theta_1 + \vartheta(\phi_\infty^2), \\ \phi &= \phi_0 + \phi_\infty \Phi_1 + \vartheta(\phi_\infty^2), \end{aligned}$$

where $\phi_0 = 0$.

The zeroth-order conservation equations for momentum and energy (heat transfer problem) in terms of u_0 , θ_0 , respectively, are those of the Blasius and Pohlhausen problems for the base fluid [9, 10]. The first-order conservation equations for u_1 , θ_1 are, respectively

$$(4.2) \quad \begin{aligned} \left(u_1 \frac{\partial u_0}{\partial x} + v_0 \frac{\partial u_0}{\partial y} \right) + \left(u_0 \frac{\partial u_1}{\partial x} + v_1 \frac{\partial u_0}{\partial y} \right) + (\rho^*)'_0 \Phi_1 \left(u_0 \frac{\partial u_0}{\partial x} + v_0 \frac{\partial u_0}{\partial y} \right) \\ \text{nanofluid inertia} \\ = \frac{1}{\text{Re}} \left(\frac{\partial^2 u_1}{\partial y^2} + (\mu^*)'_{\phi=0} \frac{\partial}{\partial y} \frac{\partial}{\partial y} \left(\Phi_1 \frac{\partial u_0}{\partial y} \right) \right), \\ \text{nanofluid viscosity} \end{aligned}$$

$$(4.3) \quad \begin{aligned} \left(u_0 \frac{\partial \theta_1}{\partial x} + v_0 \frac{\partial \theta_1}{\partial y} \right) + \left(u_1 \frac{\partial \theta_0}{\partial x} + v_1 \frac{\partial \theta_0}{\partial y} \right) + (\rho^* c^*)'_0 \Phi_1 \left(u_0 \frac{\partial \theta_0}{\partial x} + v_0 \frac{\partial \theta_0}{\partial y} \right) \\ \text{nanofluid inertia} \\ = \frac{1}{\text{Re Pr}_f} \left(\frac{\partial^2 \theta_1}{\partial y^2} + (k^*)'_{\phi=0} \frac{\partial}{\partial y} \left(\Phi_1 \frac{\partial \theta_0}{\partial y} \right) \right) + \frac{1}{\text{Re Sc}_f} \frac{\partial}{\partial y^*} \left(\rho_p^* D^* \frac{\partial \Phi_1}{\partial y^*} c_p^* \theta_0 \right). \\ \text{nanofluid conduction} \qquad \qquad \qquad \text{nanofluid diffusion energy transport} \end{aligned}$$

The nanofluid concentration equation is first-order in the nanofluid volume fraction only

$$(4.4) \quad \left(u_0 \frac{\partial \Phi_1}{\partial x} + v_0 \frac{\partial \Phi_1}{\partial y} \right) = \frac{1}{\text{Re Sc}_f} \frac{\partial}{\partial y} \left(D^* \frac{\partial \Phi_1}{\partial y} \right).$$

Recalling that the dimensionless diffusion coefficient is, for small temperature loading, $D^* \equiv 1$.

It is noticed that nanofluid inertia effects in the first-order momentum and energy equations can be recast, using the respective zeroth-order Blasius and Pohlhausen momentum and energy equations, into more compact form

$$(\rho^*)'_0 \Phi_1 \left(\frac{1}{\text{Re}} \frac{\partial^2 u_0}{\partial y^2} \right), \quad (\rho^* c^*)'_0 \Phi_1 \left(\frac{1}{\text{Re Pr}_f} \frac{\partial^2 \theta_0}{\partial y^2} \right),$$

and moved to the respective right sides,

$$(4.5) \quad \begin{aligned} \left(u_0 \frac{\partial u_1}{\partial x} + v_0 \frac{\partial u_1}{\partial y} \right) + \left(u_1 \frac{\partial u_0}{\partial x} + v_1 \frac{\partial u_0}{\partial y} \right) \\ = \frac{1}{\text{Re}} \frac{\partial^2 u_1}{\partial y^2} + \frac{1}{\text{Re}} \left[\Phi_1 \frac{\partial^2 u_0}{\partial y^2} ((\mu^*)'_{\phi=0} - (\rho^*)'_{\phi=0}) + (\mu^*)'_{\phi=0} \frac{\partial \Phi_1}{\partial y} \frac{\partial u_0}{\partial y} \right], \end{aligned}$$

$$\begin{aligned}
 (4.6) \quad & \left(u_0 \frac{\partial \theta_1}{\partial x} + v_0 \frac{\partial \theta_1}{\partial y} \right) + \left(u_1 \frac{\partial \theta_0}{\partial x} + v_1 \frac{\partial \theta_0}{\partial y} \right) \\
 & = \frac{1}{\text{Re Pr}_f} \frac{\partial^2 \theta_1}{\partial y^2} + \frac{1}{\text{Re Pr}_f} \left[\Phi_1 \frac{\partial^2 \theta_0}{\partial y^2} \left((k^*)'_{\phi=0} - (\rho^* c^*)'_{\phi=0} \right) + (k^*)'_{\phi=0} \frac{\partial \Phi_1}{\partial y} \frac{\partial \theta_0}{\partial y} \right] \\
 & \quad + \frac{1}{\text{Re Sc}_f} \frac{\partial}{\partial y^*} \left(\rho_p^* D^* \frac{\partial \Phi_1}{\partial y^*} c^* \theta_0 \right).
 \end{aligned}$$

It is now possible to render observations concerning the role of nanofluid in the advective-diffusive situation. In (4.6) and (4.7), inertia effects are moved to the right side so as to exhibit its competition with enhanced transport property of the nanofluid. In general, enhanced viscosity diffuses the velocity profile to render it less steep whereas, if $(\rho^*)'_{\phi=0} > 0$, inertia effects have the tendency of steepening the velocity profile. Similarly, enhanced thermal conductivity diffuses the temperature further and renders it less steep. Thermal inertia effects, characterized by the density-heat capacity product, because of the decrease of heat capacity in a nanofluid, tend also to stretch out the temperature as in the examples encountered $(\rho^* c^*)'_{\phi=0} < 0$, and this reinforces $(k^*)'_{\phi=0}$.

The concentration diffusion equation (4.4) stands alone, with the zeroth-order velocities given by the Blasius solution, subject to either of its wall boundary conditions in (2.10). It would be solved first so that Φ_1 now becomes a known function in solving (4.6) and (4.7).

5. Similar solutions

The first-order solutions are expressible in similarity variables, as boundary conditions permit, in the same form as the zeroth-order Blasius and Pohlhausen solutions. The correspondence between the present dimensionless variables, introduced for convenient perturbation analysis, is related to the dimensional variables found in the literature

$$\eta = \frac{y}{\sqrt{v_f x / U}} = \frac{y^*}{\sqrt{x^* / \text{Re}}}.$$

The dimensionless stream function and velocity components are related as

$$\psi^* = \frac{\psi}{UL} = \sqrt{\frac{x^*}{\text{Re}}} f(\eta), \quad u^* = f'(\eta), \quad v^* = \frac{1}{2\sqrt{x^* \text{Re}}} (\eta f' - f).$$

These are carried over to the perturbation expansions so that these relations for the zeroth- and first-order velocities are similarly related to the respective stream function of the same order. The resulting ordinary equations for $f_0 = f_{\text{Blasius}}$, f_1

are, respectively

$$(5.1) \quad f_0''' + \frac{1}{2}f_0f_0'' = 0, \quad f_0(0) = f_0'(0) = 0, \quad f_0'(\infty) = 1,$$

$$(5.2) \quad f_1''' + \frac{1}{2}(f_0f_1'' + f_1f_0'') = ((\mu^*)'_{\phi=0} - (\rho^*)'_{\phi=0})\Phi_1\frac{1}{2}f_0f_0'' + (\mu^*)'_{\phi=0}\Phi_1f_0''.$$

The boundary condition for the streamwise velocity is already satisfied by the Blasius solution, so that the first-order problem satisfies homogeneous boundary condition, it is being driven by the inhomogeneous right side of (5.2), comprising inertia effects characterized by $(\rho^*)'_{\phi=0}$ and the velocity-profile stretching or smoothing effects of enhanced viscosity characterized by $(\mu^*)'_{\phi=0}$. These two mechanisms are competing since they are of opposite sign.

The zeroth- and first-order energy equations become, after the similarity variable transformation,

$$(5.3) \quad \theta_0'' + \frac{\text{Pr}_f}{2}f_0\theta_0' = 0, \quad \theta_0 = 1, \quad \theta_0(\infty) = 0,$$

$$(5.4) \quad \theta_1'' + \frac{\text{Pr}_f}{2}(f_0\theta_1' + f_1\theta_0') = \\ - \left[((k^*)'_{\phi=0} - (\rho^*c^*)'_{\phi=0})\Phi_1\theta_0'' + (k^*)'_{\phi=0}\Phi_1\theta_0' \right] - \frac{\rho_p^*c_p^*}{\text{Sc}_f}D^*(\Phi_1'\theta_0)'.$$

The inhomogeneous equation for θ_1 satisfies homogeneous boundary conditions as the temperature boundary conditions of the problem are satisfied by θ_0 .

The nanofluid properties are dependent on the nanoparticle volume concentration, thus it is necessary to consider the volume concentration diffusion equation.

5.1. The case of a solid wall with zero nanoparticle flux

The volume diffusion problem in this case is

$$(5.5) \quad \Phi_1'' + \frac{\text{Sc}_f}{2}f_0\Phi_1' = 0, \quad \Phi_1'(0) = 0, \quad \Phi_1(\infty) = 1.$$

In the absence of sources (or sinks) in the interior of the nanofluid and on the boundaries, (5.5) yields an exact solution

$$(5.6) \quad \Phi_1(\eta; \text{Sc}_f) = 1$$

(much like the Crocco Integral for the fluid energy equation in the case of an insulated wall and $\text{Pr} = 1$, [9]). In this special case, the problem is reduced to constant thermophysical properties dependent only on the constant volume

fraction ϕ_∞ . As such, it loses the ability of regulating heat transfer at the wall via thermal energy transport through concentration diffusion according to (2.7). Thus the surface heat transfer can be ascertained from boundary layer theory using nanofluid thermophysical properties at the prevailing ϕ_∞ . This has been found to be the case in certain measurements according to PRABHAT *et al.* [19, 20], although no information on the nanoparticle volume fraction distribution is available.

5.2. The momentum and thermal problems for zero nanoparticle volume flux at solid wall

The boundary condition of zero flux at the wall produces $\Phi_1(\eta) = 1$ throughout the entire boundary layer so that $\Phi_1'(\eta) = 0$, thus (5.2) and (5.4) simplify to, respectively,

$$(5.9) \quad \begin{aligned} f_1''' + \frac{1}{2}(f_0 f_1'' + f_1 f_0'') &= ((\mu^*)'_{\phi=0} - (\rho^*)'_{\phi=0}) \frac{1}{2} f_0 f_0'', \\ f_1(0) = f_1'(0) &= 0, \quad f_1'(\infty) = 0, \end{aligned}$$

and

$$(5.10) \quad \begin{aligned} \theta_1'' + \frac{\text{Pr}f}{2}(f_0 \theta_1' + f_1 \theta_0') &= ((k^*)'_{\phi=0} - (\rho^* c^*)'_{\phi=0}) \frac{\text{Pr}f}{2} f_0 \theta_0', \\ \theta_1(0) = \theta_1(\infty) &= 0, \end{aligned}$$

where use is made of the zeroth-order momentum (5.1) and energy (5.3) equations to arrive at the “advective” form on the right sides on (5.9) and (5.10), respectively.

It is noticed that if we define

$$(5.11) \quad F_1 = f_1 / ((\mu^*)'_{\phi=0} - (\rho^*)'_{\phi=0})$$

and substitute into (5.9) to obtain

$$(5.12) \quad \begin{aligned} F_1''' + \frac{1}{2}(f_0 F_1'' + F_1 f_0'') &= \frac{1}{2} f_0 f_0'', \\ F_1(0) = F_1'(0) &= 0, \quad F_1'(\infty) = 0, \end{aligned}$$

then (5.12) can be solved for F_1 as a “universal function” independent of thermophysical properties. Less fortunate in this respect is (5.10) which requires specification of thermophysical properties prior to its solution.

5.3. Shear stress at the wall

Denoting the wall condition by the subscript 0, the Newtonian shear stress at the wall is

$$\tau_0 = \left(\mu \frac{\partial u}{\partial y} \right)_0 = \mu_f \mu_0^* u_\infty \sqrt{u_\infty / \nu_f x} f''(0),$$

the representation of the nanofluid viscosity coefficient is discussed in Section 3. Inserting the perturbation representations, to first order in ϕ_∞ , the ratio of nanofluid shear stress to that of base fluid is

$$\tau_0 / \tau_{0,f} = 1 + \phi_\infty [(\mu^*)'_{\phi=0} + f_1''(0) / f_0''(0)],$$

where base fluid shear stress is $\tau_{0,f} = \mu_f u_\infty \sqrt{u_\infty / \nu_f x} f_0''(0)$. In the similar solution for both water and for nanofluid flow, the shear stress decays as $x^{-1/2}$. The shear stress ratio or enhancement is independent of x although experimentally this may not be the case. The local skin friction coefficient is defined as the local shear stress normalized by the free stream dynamic pressure. The respective base fluid and nanofluid skin friction coefficients are

$$C_{f_f} = \tau_{0,f} / (1/2) \rho_{\infty,f} u_\infty^2, \quad C_f = \tau_0 / (1/2) \rho_{\infty,f} [1 + \phi_\infty (\rho^*)'_{\phi=0}] u_\infty^2.$$

With the appropriate definition of the skin friction coefficient, which necessarily involves the free stream density of the nanofluid, it is thus more physically straightforward to discuss the skin friction enhancement directly in terms of their ratios rather than the ratio of skin friction coefficients.

5.4. Surface heat transfer rate

The surface heat transfer rate at the wall from (2.2) includes the heat transfer owing to diffusion currents. In the present case of zero flux of nanoparticles across a solid wall for which the volume concentration is uniform, heat transfer at the wall is accomplished by heat conduction alone. Using the representation of nanofluid thermal conductivity of Section 3 and the perturbation representations, we obtain the heat transfer rate enhancement ratio, to first order in ϕ_∞

$$q_0 / q_{0,f} = 1 + \phi_\infty [(k^*)'_0 + \theta'_1 / \theta'_0(0)],$$

where the base fluid heat transfer rate is

$$q_{0,f} = k_f (T_0 - T_\infty) \theta'_0(0) \sqrt{u_\infty / \nu_f x}.$$

From the definition of the local heat transfer coefficient

$$h_x = q_0 / (T_0 - T_\infty)$$

the ratio of the surface heat transfer rates is the same as that of heat transfer coefficients

$$h_x/h_{x,f} = q_0/q_{0,f}$$

provided that the wall temperatures of the nanofluid and of the base fluid are the same.

5.5. Brief description of numerical procedure

Although the Blasius and Pohlhausen problems are well known, they are nevertheless solved to provide numerical consistency for the first-order problems. Both (5.10) and (5.11) are inhomogeneous differential equations with homogeneous boundary conditions. They are numerically solved using Octave, similar to Matlab, by writing a single function to describe the entire system $f_0, F_1, \theta_0, \theta_1$. The boundary value problem is then solved as an initial value problem by the shooting method. As there are four unknown conditions at $\eta = 0$, which are required to solve the entire system $(f_0'', F_1'', \theta_0', \theta_1')$, each of the four conditions is solved individually, one at a time. Initially, the Blasius problem is considered and forward integration is carried out in a loop as the guess for f_0'' is updated. Once the stand-alone f_0 solved, then θ_0 or F_1 may be solved in the same manner, θ_1 is solved last as the three functions are needed as variable coefficients and inhomogeneous input. The relevant code is documented but not reproduced here.

5.6. Application to specific nanofluids

For alumina $(\rho^*)'_{\phi=0,\text{mix}} = 2.89$, $(\rho^*c^*)'_{\phi=0,\text{mix}} = -0.18$. For gold-water nanofluid $(\rho^*)'_{\phi=0,\text{mix}} = 18.3$, $(\rho^*c^*)'_{\phi=0,\text{mix}} = -0.42$. Interpolating results of PULITI *et al.* [16] for heat capacity in J/mol,K to kJ/g,K via effective nanofluid molecular weight versus effective nanoparticle volume fraction, it is obtained $(\rho^*)'_{\phi=0,\text{MD}} = 18.7$, $(\rho^*c^*)'_{\phi=0,\text{MD}} = -2.37$. In the case of dilute, spherical nanoparticles, the nanofluid behaves like a Newtonian fluid, Einstein's result $(\mu^*)'_{\phi=0,\text{Einstein}} = 2.5$ is satisfactory. The classical result of Maxwell gives $(k^*)'_{\phi=0,\text{Maxwell}} = 3$, but WEN and DING'S [2] measurements give $(k^*)'_{\phi=0,\text{W\&D}} \cong 6$ for water-based alumina.

Molecular dynamics simulation for viscosity and thermal conductivity of gold nanoparticles appear only in the thesis of PULITI [15] and are subject to interpretation to bring the results into practical form. The results suggest that $0 \leq (\mu^*)'_{\phi=0,\text{MD}} \leq 10$ based on points for $\phi = 0$ and $\phi = 0.10$, including the full expanse of error bars [15, Fig. 3.30 and Table 3.3). There are, however some doubts engendered by the incorrect value produced by the simulation for pure water at $\phi = 0$ and the negative slope of the computed value of $(\mu^*)'_{\phi=0,\text{MD}}$ at $\phi = 0.01$. The molecular dynamics result for gold nanoparticle thermal conduc-

tivity [15] suggests that $(k^*)'_{\phi=0,MD} = 4.3$ between $\phi = 0$ and $\phi = 0.10$; but for small concentrations to $\phi = 0.01$, $(k^*)'_{\phi=0,MD} \leq 20$. The summary of properties values in applications are given in the following table

Case I. Alumina, mix	Case II. Gold-Water, mix	Case III. Gold-Water, MD
$(\rho^*)'_{\phi=0,mix} = 2.89$	$(\rho^*)'_{\phi=0,mix} = 18.3$	$(\rho^*)'_{\phi=0,MD} = 18.7$
$(\rho^*c^*)'_{\phi=0,mix} = -0.18$	$(\rho^*c^*)'_{\phi=0,mix} = -0.42$	$(\rho^*c^*)'_{\phi=0,MD} = -2.37$
$(\mu^*)'_{\phi=0,Einstein} = 2.5$	$(\mu^*)'_{\phi=0,Einstein} = 2.5$	$(\mu^*)'_{\phi=0,MD} = 10$
$(k^*)'_{\phi=0,W\&D} \cong 6$	$(k^*)'_{\phi=0,Maxwell} = 3$	$(k^*)'_{\phi=0,MD} = 20$

The thermophysical properties representing the competition between conductive, diffusive effects and advective effects of inertia are reproduced below

	Case I	Case II	Case III
	Alumina, mix	Gold-Water, mix	Gold-Water, MD
$(\mu^*)'_{\phi=0} - (\rho^*)'_{\phi=0}$:	-0.39	-15.80	-8.70
$(k^*)'_{\phi=0} - (\rho^*c^*)'_{\phi=0}$:	+6.18	+3.42	+22.37

6. The normalized universal velocity function

The universal function $F'_1(\eta)$ from (5.12) is the first-order velocity function, normalized by material properties as indicated, is shown in Fig. 1 together with the zeroth-order Blasius velocity function f'_0 of (5.1).

The first-order velocity profile decreases the steepness of the Blasius velocity profile as increasing function of the volume fraction as the stretching factors are

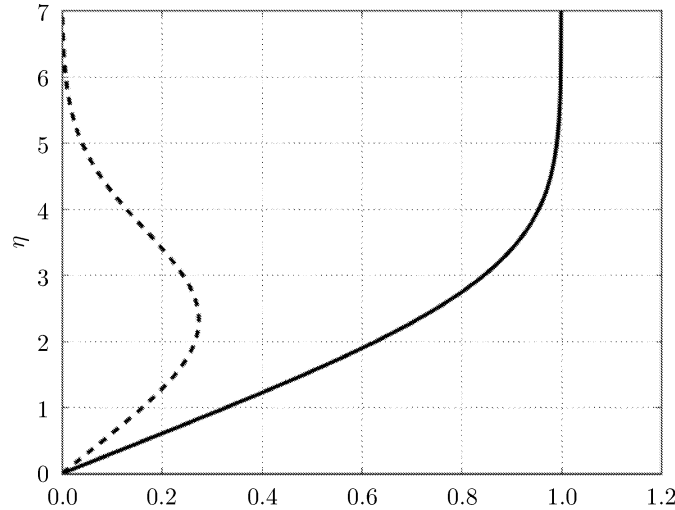


FIG. 1. The first-order universal velocity function F'_1 ----, the zeroth-order Blasius velocity function f'_0 — vs. the Blasius similarity variable η , where $F_1 = f_1/((\mu^*)'_{\phi=0} - (\rho^*)'_{\phi=0})$.

negative for all three cases considered. The enhanced viscosity effect is to stretch the velocity profile rendering it less steep, whereas the inertia effect is to steepen the velocity profile. The imbalance of these two effects, according to the material properties obtained, is to decrease the steepness of the overall velocity profile.

7. Specific cases of application: velocity and temperature profiles

7.1. Case I: alumina-water nanofluid

The nanofluid effects on the velocity profiles is best brought out by the difference between the nanofluid velocity and that of the base fluid Blasius profile, in terms of the universal velocity function,

$$[f'(\eta) - f'_0(\eta)]/\phi_\infty = f'_1(\eta) = ((\mu^*)'_{\phi=0} - (\rho^*)'_{\phi=0})F'_1(\eta),$$

$$((\mu^*)'_{\phi=0} - (\rho^*)'_{\phi=0}) = -0.39$$

The modification of nanofluid velocity profile over that of the base fluid conceivably could be measured in laboratory experiments. In Fig. 2 is shown the velocity profile difference for Case I for small volume fraction.

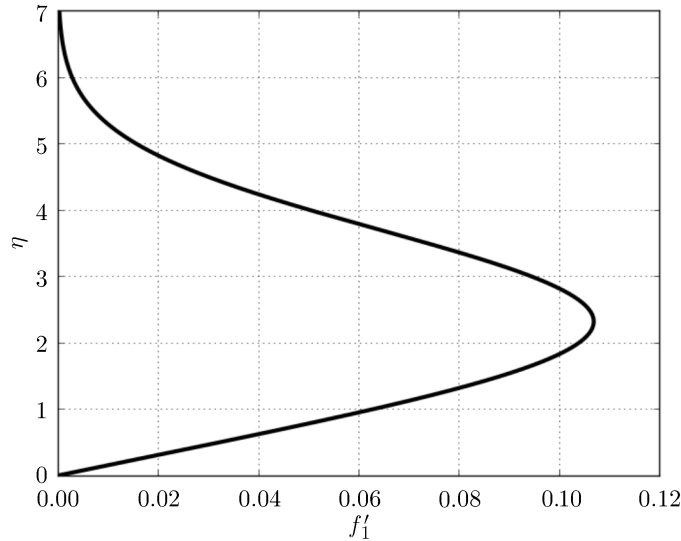


FIG. 2. The first-order velocity profile $f'_1(\eta)$ for alumina-water nanofluid as function of the similarity variable η , Case I.

The maximum value of $f'_1(\eta) = \vartheta(0.1)$ so that for small volume fraction the over all profile would be graphically difficult to visualize, although the profile $f'_1(\eta)$ itself is numerically discernable.

The temperature profiles from (5.10) need the input of property values in their solution as well as the velocity profiles. The case for alumina is shown in Fig. 3 (Case I). In this case the overall temperature profile

$$\theta(\eta) = \theta_0(\eta) + \phi_\infty \theta_1(\eta)$$

is rendered less steep with increasing volume fraction. In the much simpler case of Rayleigh–Stokes approximation [1], it was pointed out, as with the velocity profile, there is the competition between the profile stretching effect of enhanced transport property (thermal conductivity in this case) and the temperature profile steepening effect of inertia through the density–heat capacity product. It is more intricate in the boundary layer problem here than in the thermal Rayleigh–Stokes problem [1] as the velocity profiles are also involved, as (5.10) clearly shows. Again, the nanofluid temperature profile effect is best shown as the difference between nanofluid temperature and that of the base fluid which correspond to the Pohlhausen profile [10]

$$[\theta(\eta) - \theta_0(\eta)]/\phi_\infty = \theta_1(\eta),$$

and this, again, could be measured in the laboratory. The maximum value of the first-order temperature profile is about 1.1 (Fig. 3).

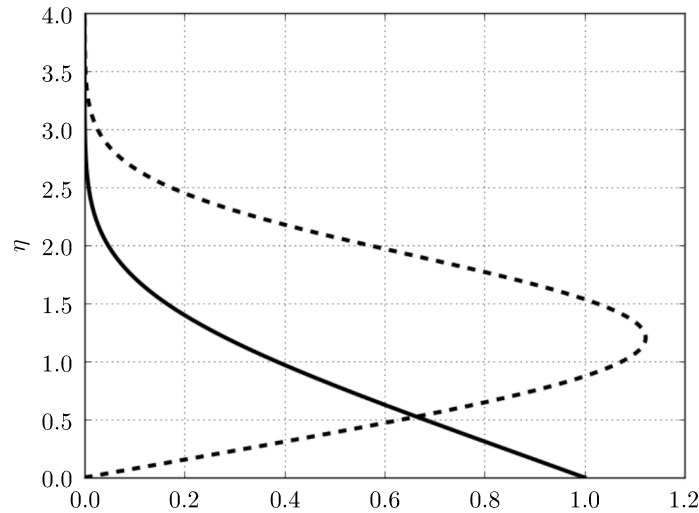


FIG. 3. The zeroth-order Pohlhausen profile θ_0 —, first-order temperature profile θ_1 ---- as function of the similarity variable, η alumina-water (Case I), $\text{Pr}_f = 7$.

7.2. Case II: Gold-water nanofluid (mix)

The first-order perturbation velocity profile for Case II is

$$[f'(\eta) - f'_0(\eta)]/\phi_\infty = f'_1(\eta) = ((\mu^*)'_{\phi=0} - (\rho^*)'_{\phi=0})F'_1(\eta),$$

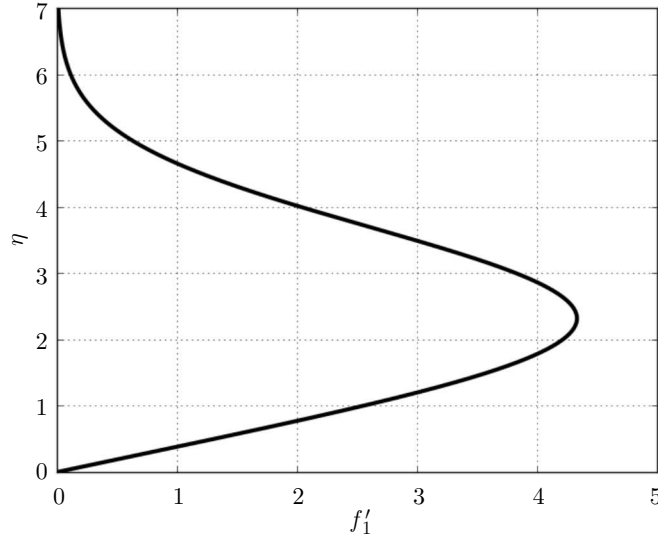


FIG. 4. First-order velocity profile $f'_1(\eta) = ((\mu^*)'_{\phi=0} - (\rho^*)'_{\phi=0})F'_1(\eta)$, as function of the similarity variable η , Case II.

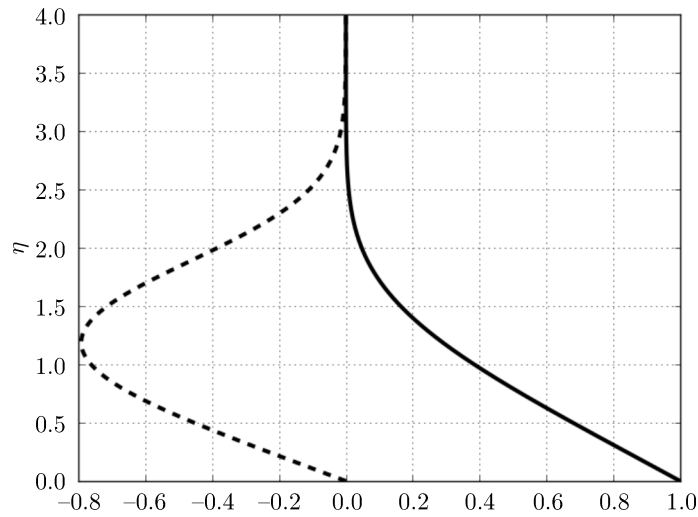


FIG. 5. Gold-water nanofluid temperature profiles vs. similarity variable η , Case II. First-order profile $\theta_1(\eta)$ ---- is negative and is shown on the left, the zeroth-order Pohlhausen profile is on the right θ_0 —, $Pr_f = 7$.

where $(\mu^*)'_{\phi=0} - (\rho^*)'_{\phi=0} = -15.80$, is shown in Fig. 4. It has a maximum value greater than 4.0 and is significantly greater than that for Case I. It gives rise to a steepening of the overall velocity profile.

The first-order temperature profile $\theta_1(\eta)$ for Case II is shown in Fig. 5, along with the zeroth-order Pohlhausen profile. In this case, the nanofluid effect is to steepen the dimensionless temperature gradient at the wall. The maximum magnitude of $\theta_1(\eta)$ is about -0.8 and again, $[\theta(\eta) - \theta_0(\eta)]/\phi_\infty = \theta_1(\eta)$ appears to be a measurable quantity.

7.3. Gold-water nanofluid (MD) Case III

The velocity difference profile for Case III,

$$\begin{aligned} [f'(\eta) - f'_0(\eta)]/\phi_\infty &= f'_1(\eta) = ((\mu^*)'_{\phi=0} - (\rho^*)'_{\phi=0})F'_1(\eta), \\ ((\mu^*)'_{\phi=0} - (\rho^*)'_{\phi=0}) &= -8.70, \end{aligned}$$

is shown in Fig. 6, with a maximum value of about 2.4. It again contributes to the steepening of the overall velocity profile.

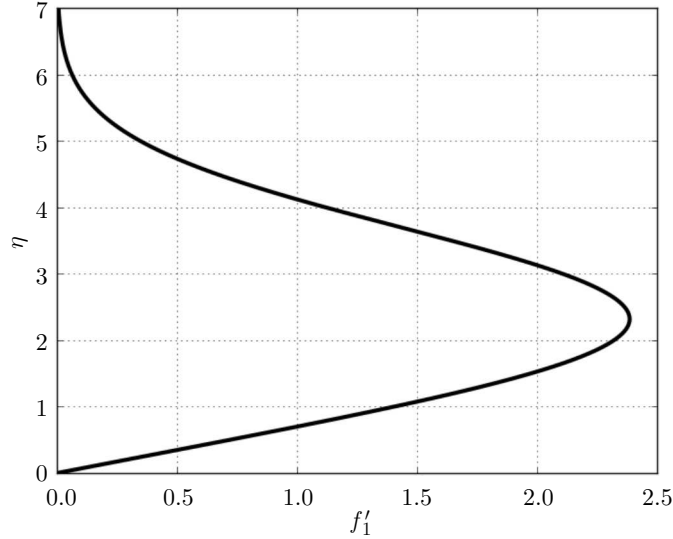


FIG. 6. The first-order velocity profile $f'_1(\eta) = ((\mu^*)'_{\phi=0} - (\rho^*)'_{\phi=0})F'_1(\eta)$ for Gold-water nanofluid. Case III.

The first-order temperature profile for Case III,

$$[\theta(\eta) - \theta_0(\eta)]/\phi_\infty = \theta_1(\eta)$$

is shown in Fig. 7, with a maximum value about 3.4. The nanofluid effect of the temperature profile is to decrease the gradient at the wall. Although not obvious

in the boundary layer problem, the Rayleigh–Stokes problem [1] tells us that it is attributable to the large thermal conductivity effect of smoothing out the temperature profile.

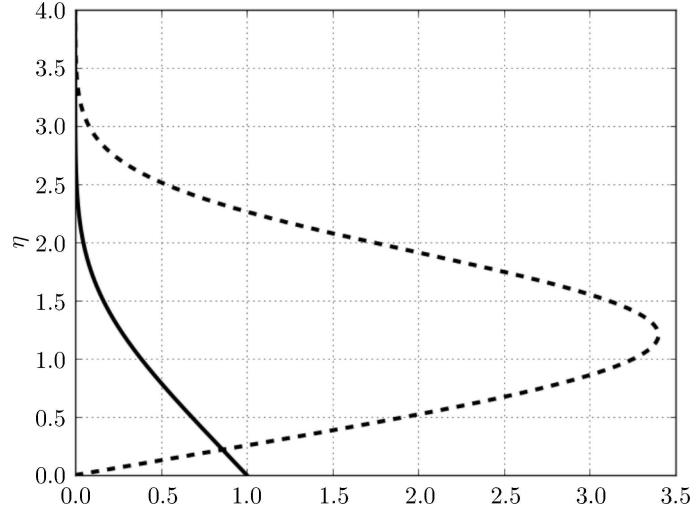


FIG. 7. Gold-water (MD) nanofluid temperature profiles vs. similarity variable η , Case III. First-order profile $\theta_1(\eta)$ ---- is positive, the zeroth-order Pohlhausen profile θ_0 —, $\text{Pr}_f = 7$.

8. Surface heat transfer rate and skin friction

In the previous section the nanofluid effects on the velocity and temperature profiles are illustrated, owing to the next effect of steepening due to inertia and profile stretching effects of enhanced transport properties. The impact of transport effects on the resulting velocity and temperature profiles are discussed in this section and has an explicit effect on the enhancement of nanofluid skin friction rise and heat transfer relative to the base fluid, overcoming the profile-stretching effects of enhanced nanofluid transport properties in the respective conservation equations of momentum and static enthalpy.

The general relations for skin friction and surface heat transfer rate are rewritten in terms of relations normalized by the corresponding values of the base fluid. The relative skin friction enhancement is, to first order in ϕ_∞

$$\tau^* - 1 = \phi_\infty [(\mu^*)'_{\phi=0} + f_1''(0)/f_0''(0)] = \phi_\infty (\tau^*)'_{\phi=0},$$

where $\tau^* = \tau_0/\tau_{0,f}$ and the base fluid shear stress is $\tau_{0,f} = \mu_f u_\infty \sqrt{u_\infty/v_f x} f_0''(0)$. The slope $(\tau^*)'_{\phi=0}$ requires the input of transport property and the solution of the boundary layer similarity solutions up to the first order.

The heat transfer rate at the wall for zero flux of nanoparticles across the wall is accomplished by heat conduction alone. Using the representation of nanofluid thermal conductivity and the perturbation representations, we obtain the enhanced heat transfer rate relative to the base fluid, to first order in ϕ_∞

$$q^* - 1 = \phi_\infty [(k^*)'_0 + \theta'_1(0)/\theta'_0(0)] = \phi_\infty (q^*)'_{\phi=0},$$

where the surface heat transfer rate is normalized by that of the base fluid

$$q^* = q_0/q_{0,f}, \quad q_{0,f} = k_f(T_0 - T_\infty)\theta'_0(0)\sqrt{u_\infty v_f x}.$$

The results in the rise in shear stress and heat transfer enhancement are presented in the following table, for the three cases discussed.

	Case I alumina (mix)	Case II gold/water (mix)	Case III gold/water (MD)
$(q^*)'_{\phi=0}$	3.98	4.44	13.90
$(\tau^*)'_{\phi=0}$	2.70	10.40	14.35

8.1. Case I

The comparisons with experiments in alumina-water nanofluids (Case I) are made for the highest Reynolds numbers. This ensures that the measurements are in the entrance region of channels [3] and tubes [4], which corresponds to the present boundary layer region rather than in the developed region. The comparisons are shown here in terms q^* of in Fig. 8 and 9, respectively. The theory from use of mixture properties under estimates measurements.

The underestimation by the theory of experimental enhancement in the entrance region can be attributed to several factors. One is believed to be the

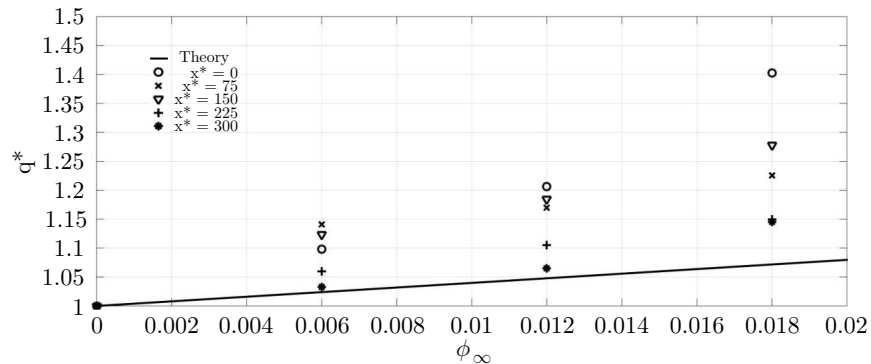


FIG. 8. Comparison of theory (mix) for alumina-water nanofluids, measurements are those of JUNG *et al.* [3] at Reynolds number of 287 (characteristic length based on channel height).

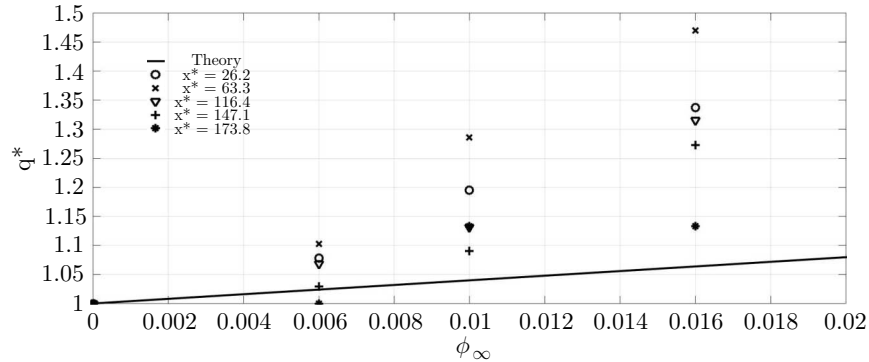


FIG. 9. Comparison of theory (mix) for alumina-water nanofluids, measurements are those of WEN and DING [2] at Reynolds number of 1600 (characteristic length based on tube diameter).

use of mixture and “conventional” thermophysical properties which consistently underestimate the heat transfer enhancement from that of experiments. (MD calculation of thermophysical properties for alumina-water is not available). The other reasons are that the upstream detailed initial conditions of nanofluid velocity and temperature in the experiments are not known. The entrance of channels and tubes are fed by tubes which most certainly has developed velocity and temperature profiles which advects flow and temperature in the experimental channels or tubes. The measurements all indicate a high degree of non-similarity in the streamwise development from the entrance leading edge. Experimental results contrast with theory, which assumes uniform entrance region velocity and temperature which allowed the simplicity of similar solutions. In this case, the theory gives a minimum level of enhancement and forms the basis for further extensions into realistic thermophysical properties, when available, and more realistic upstream conditions based upon experimentation.

The relative heat transfer enhancement and skin friction rise for Case I is shown in Fig. 10.

The Case I result, according to the boundary layer solution and the use of thermophysical properties stated, actually give rise to a relative larger heat transfer enhancement than the rise in skin friction, a scenario more optimistic than that described in [14]. This is because of the leading edge effects in the present theory, which accounts for the inertia effects, the nanofluid density in momentum convection and the nanofluid density-heat capacity in the convection of static enthalpy. If one were to consider fully developed flow, where no such convection effects are present, would give a pessimistic account of nanofluids in heat transfer enhancement. In fact, DING *et al.* [21] proposed heat exchanger using an assembly of entrance region heat transfer tubes or channels. The present

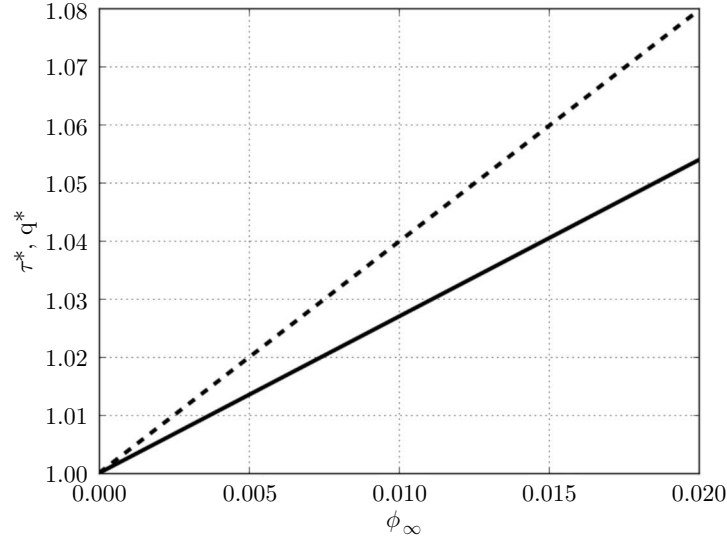


FIG. 10. Heat transfer enhancement and skin friction rise vs. volume fraction. Case I, alumina-water(mix) nanofluid; q^* ----, τ^* —.

analysis and of LIU [1], which brought out the completion between inertia effects and enhanced transport effect in the stretching or squashing of the temperature profile and velocity profiles, which in turn, augment the explicit transport effect in the surface heat transfer rate and skin friction. This emphasize that transport properties play a dual, opposing role when convection effects are present.

8.2. Gold nanofluid (mix), Case II

Although there are no experiments performed with gold nanoparticles, there exist (MD) calculations [15–17] of properties. The results of their use in boundary layer analysis can be compared to that from mixture calculation (mix) of properties and conventional transport properties. The profile results, Figs. 4 and 5, which reflects the competition between nanofluid convection and diffusive effects on the profiles, together the surface hear transfer rate and skin friction rise, reflecting the enhance nanofluid transport properties, as in Fig. 10 for Case I, are given in Fig. 11 for Case II.

8.3. Gold nanofluid, Case III

The corresponding surface heat transfer rate and skin friction rise for Case III is shown in Fig. 12.

The results from Figs. 11 and 12, Cases II and III, respectively, indicate that mixture approach and conventional use of Einstein and Maxwell viscosity and

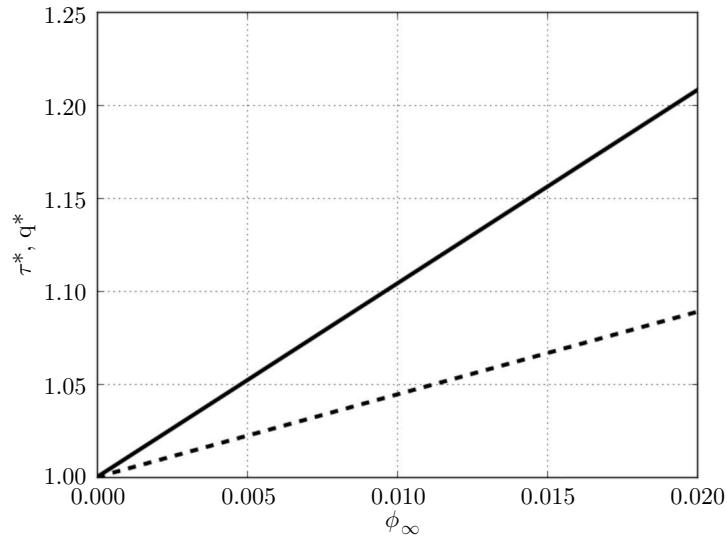


FIG. 11. Heat transfer enhancement and skin friction rise vs. volume fraction. Case II, gold-water (mix) nanofluid; q^* ----, τ^* —.

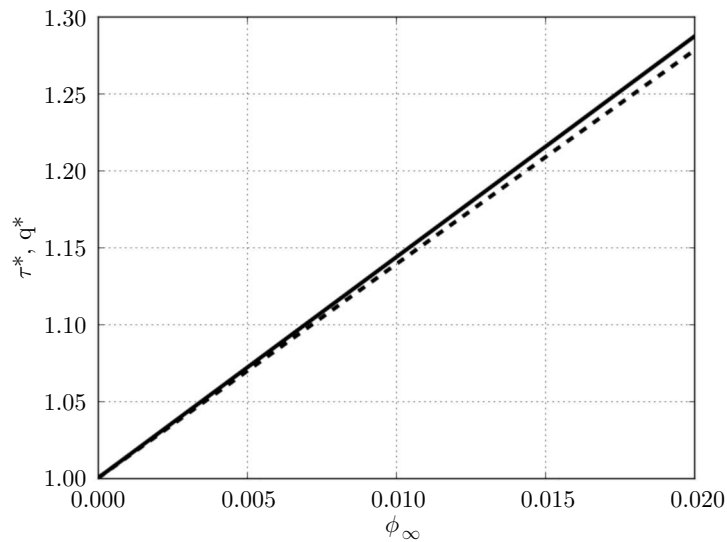


FIG. 12. Heat transfer enhancement and skin friction rise vs. volume fraction. Case III, gold-water (MD) nanofluid; q^* ----, τ^* —.

thermal conductivity relations considerably underestimates both the skin friction rise and enhanced heat transfer compared to molecular dynamics results for thermophysical properties. Use of molecular dynamics obtained [15–17] thermophysical properties in the present boundary layer theory appreciably enhanced

both the surface heat transfer rates and skin friction. The relative enhancements are very nearly one-to-one (Fig. 12) and thus removes the pessimism expressed in [14] concerning nanofluids, at least for gold-water nanofluids. Also, their [14] conclusion is based largely on fully developed flow which does not have the benefit of the developing leading effect of bring into play convective inertia effects [1–3, 21] which is brought out by the present work.

8.4. Remarks on gold nanofluid experiments

An experimental study of convective heat transfer of gold-water nanofluid in a tube of diameter 2.27 mm and 580 mm length is reported by SABIR *et al.* [22]. As in experiments [2,3] designed for heat transfer studies, the entrance velocity and temperature profiles are not well defined. The reported [22] enhanced surface heat transfer rate q^* , in terms of the present notation, attained values of 1.08, 1.15 and 1.23 for nanofluid volume fraction of 0.00015, 0.00045 and 0.000667, respectively. In this case, data points would almost appear along the vertical axis in Fig. 12 for these unusually minute volume fractions. The thermal conductivity is not explicitly presented in these specific experiments [22]. Thus it is difficult to uncover whether the thermal conductivity enhancement mechanism falls within and aligned with the extensive measurements discussed in [13].

9. Concluding remarks

It is found that the use of molecular dynamics properties for gold-water nanofluids considerably increased the heat transfer enhancement relative to results using “conventional” properties. Furthermore, heat transfer enhancement is comparable to the enhanced skin friction rise, whereas using conventionally obtained properties the enhanced skin friction rise is ominously larger than the heat transfer enhanced for gold nanoparticles. To fully appreciate the potential in the use of nanofluids in heat transfer enhancement, further molecular dynamics computations of properties of nanofluids, including transport properties, accompanied by careful laboratory experiments on velocity and temperature profiles are thus suggested. Possible theoretical extensions would be to include upstream shear flows prior to the leading edge problem, as would be found in experimental heat transfer measurements where the microchannels and tubes are fed by upstream nanofluid in tubes.

Acknowledgements

JTCL expresses his thanks and gratitude to the Department of Mechanics and Physics of Fluids, IPPT-PAN, in particular, Tomasz Kowalewski, as well as

his colleagues, for the stimulating hospitality during my sabbatical leave when much of the manuscript was prepared. The material is the partial subject of a seminar at IPPT on November 9, 2015. Fond remembrances of my late friends Władysław Fiszdon, Henryk Zorski, Ryszard Herczyński of IPPT are respectfully expressed.

References

1. J.T.C. LIU, *On the anomalous laminar heat transfer intensification in developing region of nanofluid flow in channels or tubes*, Proc. R. Soc. A. **468**, 2383–2398, 2012 (doi:10.1098/rspa.2011.0671).
2. D. WEN, Y. DING, *Experimental investigation into convective heat transfer of nanofluids at the entrance region under laminar flow conditions*, Int. J. Heat Mass Transfer, **47**, 5181–5188, 2004 (doi:10.1016/j.ijheatmasstransfer.2004.07.012).
3. J.-Y. JUNG, H.-S. OH, H.-Y. KWAK, *Forced convective heat transfer of nanofluids in micro channels*, Int. J. Heat Mass Transfer, **52**, 466–472, 2009 (doi:10.1016/j.ijheatmasstransfer.2008.03.033).
4. J. BUONGIORNO, *Convective transport in nanofluids*, ASME J. Heat Transfer, **128**, 240–250, 2006 (doi:10.1115/1.2150834).
5. R.B. BIRD, W.E. STEWART, E.N. LIGHTFOOT, *Transport Phenomena*, 2nd ed., Hoboken, N.J., Wiley, 2001.
6. R.F. PROBSTEIN, *Physicochemical Hydrodynamics: An Introduction*, 2nd ed., Hoboken, N.J., Wiley, 2003.
7. J.O. HIRSCHFELDER, C.F. CURTISS, R.B. BIRD, *Molecular Theory of Gases and Liquids*, Hoboken, N.J., Wiley, 1964.
8. E. PFAUTSCH, *Forced convection in nanofluids over a flat plate*, M.Sc. Thesis, University of Missouri, 2008.
9. H. SCHLICHTING, *Boundary Layer Theory*, 7th ed. (transl. J. Kestin), NY, McGraw Hill, 1979.
10. E. POHLHAUSEN, *Der Wärmeaustausch zwischen festen Körpern und Flüssigkeiten mit kleiner Reibung und kleiner Wärmeleitung*, Z. A. M. M. **1**, 115–121, 1921 (doi:10.1002/zamm.19210010205).
11. L. LEES, *Laminar heat transfer over blunt nose bodies at hypersonic flight speeds*, Jet Propulsion J. ARS., **26**, 259–269, 274, 1956 (doi:10.2514/8.6977).
12. P.A. LAGERSTROM, *Laminar Flow Theory*, Princeton Univ. Press, 1996.
13. J. BUONGIORNO *et al.*, *A benchmark study on the thermal conductivity of nanofluids*, J. Appl. Phys., **106**, 094312, 2009 (doi:10.1063/1.3245330).
14. D.C. VENERUS *et al.*, *Viscosity measurements on colloidal dispersions (nanofluids) for heat transfer applications*, Appl. Rheol., **20**, 44582-1-44582-7, 2010.
15. G. PULITI, *Properties of Gold-Water Nanofluids Using Molecular Dynamics*, PhD Thesis, Univ. Notre Dame, 2012.

16. G. PULITI, S. PAOLUCCI, M. SEN, *Thermodynamic properties of gold-water nanofluids using molecular dynamics*, *J. Nanopart. Res.*, **14**, 1296, 2012 (doi: 10.1007/s11051-012-1296-4).
17. S. PAOLUCCI, G. PULITI, *Properties of nanofluids*, *Heat Transfer Enhancement with Nanofluids*, V. Bianco, O. Manca, S. Nardini & K. Vafai [Eds.], N.Y.: CRC., 1–44, 2015.
18. H. CHEN, Y. DING, *Heat transfer and rheological behavior of nanofluids – A review*, *Advances in Transport Phenomena*, **1**, 135–177, L.Q. Wang [Ed.], Heidelberg, Springer, 2009.
19. N. PRABHAT, J. BUONGIORNO, L.-W. HU, *A critical evaluation of anomalous convective heat transfer enhancement in nanofluids*, [in:] *Abstract in Nanofluids: Fundamentals and Applications II*, 15–19 August 2010, Montréal. New York, 2010; (also as N. Prabhat, M.S. Thesis, Department of Nuclear Science and Engineering, MIT, <http://libguides.mit.edu/diss>), 2010.
20. N. PRABHAT, J. BUONGIORNO, L.-W. HU, *Convective heat transfer enhancement in nanofluids: real anomaly or analysis artifact?*, [in:] *Proc. ASME/JSME 2011 8th Thermal Engineering Joint Conf.*, 13–17 March 2011, Honolulu. Paper No. AJTEC2011-44020, 2011.
21. Y. DING *et al.*, *Heat transfer intensification using nanofluids*, *KONA*, no. 25, 23–38, 2007.
22. R. SABIR, N. RAMZAN, A. UMER, H. MURYAM, *An experimental study of forced convection heat transfer characteristic of gold water nanofluid in laminar flow*, *Sci. Int. (Lahore)*, **27**, 235–241, 2015.

Received August 8, 2016; revised version January 3, 2017.
